ELSEVIER

Journal of Nuclear Materials 307–311 (2002) 1563–1567

journal of nuclear materials

www.elsevier.com/locate/jnucmat

Structural and mechanical properties of welded joints of reduced activation martensitic steels

G. Filacchioni [a,*], R. Montanari [b], M.E. Tata [b], L. Pilloni [a]

[a] *ENEA, New Materials Division, Technologies and Materials Qualification Section, CR Casaccia, Via Anguillarese 301, I-00060 S.M. di Galeria, Rome, Italy*

[b] *INFM, Department of Mechanical Engineering, University of Rome-Tor Vergata, Via di Tor Vergata 110, I-00133 Rome, Italy*

Abstract

Gas tungsten arc welding and electron beam welding methods were used to realise welding pools on plates of reduced activation martensitic steels. Structural and mechanical features of these simulated joints have been investigated in as-welded and post-welding heat-treated conditions. The research allowed to assess how each welding technique affects the original mechanical properties of materials and to find suitable post-welding heat treatments. This paper reports results from experimental activities on BATMAN II and F82H mod. steels carried out in the frame of the European Blanket Project – Structural Materials Program.

1. Introduction

A detailed design of a magnetic fusion reactor machine has been not yet realised but most likely that complex plant will be constituted by components manufactured with different methods, like forged, mechanically machined and welded parts. Welded joints are generally known as potential 'weakest links' of a structure, thus weldability of the selected structural alloys becomes a compulsory requirement.

At present, the reduced activation ferrous (RAF) alloys are candidates for structural applications in a Tokamak reactor. RAF alloys appear as a promising choice because they are tougher than conventional martensitic steels and seem to be less sensitive to hardening, loss of tenacity and increase of ductile to brittle transition temperature (DBTT) under irradiation [1–3].

The knowledge of their weldability is still insufficient even if interesting results about F82H mod. [4–6], JLF-1 [7] and OPTIFER-IV [8] have been recently published.

Final and safe design needs sound data from extended and deepened experimental activities. For that reason, in 1998 a program started aimed to enlarge the knowledge about the weldability of RAF steels. Welded joints of Ti-bearing steels (BATMAN II alloys [9,10]) and of F82H mod. were realised and their structural features and mechanical behaviour were investigated. The final goal was to check how mechanical properties change across the joints and to find the post-welding heat-treated (PWHT) which best approaches the original characteristics. The optimisation of PWHT is of particular importance for reducing the DBTT in irradiated joints as demonstrated by the experiments of Rensman et al. [6].

2. Materials and experimental

2.1. Characteristics of the base materials

The investigated materials are representative of the RAF alloys presently under development. They belong to the group of 7–9% Cr, 1–2% W, 0.2 % V (Ta or

* Corresponding author: Tel.: +39-06 30483142; fax: +39-06 30484864.

E-mail address: gianni.filacchioni@casaccia.enea.it (G. Filacchioni).

0022-3115/02/$ - see front matter © 2002 Elsevier Science B.V. All rights reserved.
PII: S0022-3115(02)01073-5

Table 1
Chemical compositions of the investigated steels (wt%)

Alloy	C	Cr	Si	Mn	Ni	Mo	W	V	Nb	Ta	Ti	B[a]	N[a]
BATMAN IIA[b]	0.12	8.45	0.03	1.34	0.02	0.02	1.45	0.17	0.01	–	0.12	70	70
BATMAN IID[b]	0.13	7.55	0.03	0.52	0.02	0.02	1.41	0.20	0.01	–	0.07	57	41
BATMAN IIC[b]	0.12	8.67	0.02	0.52	0.02	0.02	1.43	0.2	0.01	–	0.07	64	57
F82H mod.	0.09	7.67	0.11	0.16	0.02	0.01	1.96	0.16	–	0.02	0.01	10	50

[a] The amount is expressed in p.p.m.
[b] Elsewhere [9,10] BATMAN IIA was identified as cast no. 1951, BATMAN IIC as cast no. 1955, BATMAN IID as cast no. 1953.

Table 2
Heat treatments and mechanical properties of the investigated steels

Alloy	Austenitization	Tempering	Grain size ASTM no.	HV (kg/mm^2)	0.2 YS (MPa)	UTS (MPa)	Total elongation A (%)	Reduction of area Z (%)
BATMAN IIA	1020 °C, 1 h	730 °C, 1h	~9	221	506	658	26	77
BATMAN IID	1020 °C, 1 h + 1020 °C, 1 h	730 °C, 1h	~10	222	524	670	25	78
BATMAN IIC	1020 °C, 1 h + 1020 °C, 1 h	730 °C, 1h	~10	218	524	668	24	77
F82H mod.	1040 °C, 40 min	760 °C, 1h	~4	210	520	650	23	78

Ti-stabilised) steels and are among the E.U. candidates for structural applications in blanket. F82H mod. alloy has been the first attempt to realise an industrial quantity of RA steel (a 5-tons cast was produced). The other alloys are experimental heats produced in 70–100 kg ingots. All materials showed a fully martensitic structure, the presence of δ-ferrite islands has not been evidenced.

The chemical compositions of the examined steels and some relevant data regarding heat treatments and mechanical properties are reported in Tables 1 and 2.

2.2. Welding procedures and post-welding heat treatments

Welding pools were realised, without pre-heating, on 7.5-mm thick plates of F82H mod. and on 5-mm thick plates of BATMAN II steels by gas tungsten arc welding (GTAW) and electron beam welding (EBW) methods. In both cases, the plates have been rigidly clamped to a massive aluminium support to impose a severe constraint condition.

All the simulated GTA welded joints were made with torch current of 180 A, voltage of 12 V; torch speed of 120 mm/min and the molten pool was protected by an argon flow. For EBW the beam had a voltage of 60 kV. A current of 57 mA was used for the 5 mm thick plates while 90 mA were applied for thicker products. All the EB welded pools crossed the plate.

To find the best PWHT conditions, the welded joints were submitted to treatments performed in a temperature range of ±30 °C around the temperature of the 'standard' tempering treatment for times of 0.5 and 1 h.

2.3. Structural and mechanical characterisation

Each weld was transversally sectioned, mechanically polished, etched by Vilella reagent, and then observed by optical microscopy at low and high magnification. The morphology and the extent of the molten (MZ) and heat affected zones (HAZ) were analysed. Carbide precipitation induced by welding was also studied. Portions of the weld corresponding to the MZ were cut and then electrochemically dissolved. The electrochemical method employed a cell operating at room temperature with a solution of HCl (10%) in methanol, a stainless steel cathode, tension was 1.5 V and current 0.5 A. The filtering was performed using Durapore membrane with pores of 0.1 μm. The extracted particles were analysed by X-ray diffractometry (XRD). XRD spectra have been recorded by step scanning the 2Θ angular range 15–35° with steps of 0.05° and counting times of 5 s. Mo–Kα radiation ($\lambda = 0.07093$ nm) was used.

Before and after PWHT, the properties of all joints have been studied by means of Vickers microhardness measurements (load = 0.1 kgf) performed in the same cross-section used for metallographic observations. GTAW joints were also investigated by flat-top indenter for mechanical characterisation (FIMEC) tests. The FIMEC test is based on the penetration, at constant rate, of a flat WC punch of small size ($\Phi = 1$ mm, $h = 1.5$ mm). During the test the applied load (q) and the penetration depth (δ) are measured and recorded. From these data it is possible to determine stress vs. penetration depth curves by dividing loads by the punch-surface contact area A ($A = \pi(\Phi/2)^2 \simeq 0.785$ mm^2). The char-

acteristics of these curves have been described in detail in previous works [11,12]: the limit value q_Y is reached after an initial linear stage, which is followed by a work hardening stage tending to saturation. In certain standardised conditions (penetration rate $\simeq$0.1 mm/min and deformation rate in tensile test $\simeq 10^{-3}$ s^{-1}), $q_Y \simeq 3\sigma_Y$ being σ_Y the yield stress (0.2% YS). So, the local value of yield stress has been determined directly in the MZ of GTAW joints. Unfortunately, it was not possible to perform such measurements on EB welds because they are too narrow.

3. Results and discussion

The micrographs of Fig. 1(a) and (b) show the GTA (a) and EB (b) welded pools in BATMAN IID and are representative also of the other investigated steels. The MZ produced by the torch in GTAW appear like circular sectors with depths ranging from 2 to 2.4 mm, the aspect ratios (depth/width) range from 0.22 to 0.26. The minor penetration was measured on the high manganese BATMAN IIA steel. The molten regions are surrounded by the HAZ having a nearly constant width, about 0.78 mm for the BATMAN steels and 0.95 mm for F82H mod. steel.

EB welds exhibit a classical nail-like aspect in all steels. The MZ head has a maximum width ranging between 2.9 and 3.7 mm and the maximum HAZ extent was found at the root of the nail stem ($\sim$0.7 mm for any material).

Fig. 1(c) shows the martensitic structure of the MZ in BATMAN IID (GTAW in Fig. 1(a): laths form packets inside prior austenitic grains, which generally have mean size slightly larger than that of the base material. All the examined steels exhibit similar features in MZ no matter the welding technique. Both GTAW and EB welded pools seem free from δ-ferrite islands.

XRD analysis on particles extracted from the MZ of welds evidenced the presence of different types of carbides, in particular of the Cr-rich carbides M_7C_3 and $M_{23}C_6$ (M = Cr, Fe). The relative amounts of Cr-rich carbides depend on the technique of welding because GTAW and EB involve different thermal gradients during cooling. Since M_7C_3 and $M_{23}C_6$ precipitate in the joint when the metal is cooled down to room temperature, their relative quantities are strictly connected to the cooling rate. For example, XRD patterns of particles taken from the MZ of GTA and EB welds of F82H mod. steel are displayed in Fig. 2. Five different types of carbides have been identified: M_7C_3, $M_{23}C_6$, W_2C, V_2C and Fe_6W_6C. In both welds, the reflections of M_7C_3 are the more intense; those of $M_{23}C_6$ are somewhat reduced but still clearly visible in GTA weld whereas in EB weld they are so weak to approach the detectability limit. The lesser relative quantity of $M_{23}C_6$ found in MZ of electron beam weld is linked to the faster cooling of metal: the temperature range at which $M_{23}C_6$ precipitate (600–750 °C) is crossed too quickly.

To find the optimal conditions for PWHT, the welds were heated for 0.5 and 1 h at different temperatures in a range of ±30 °C around that of standard tempering, and then microhardness measurements were carried out across the joints. The trends have been compared with those obtained before each treatment. Typical trends are shown in Fig. 3 for an EB weld of BATMAN IIA steel.

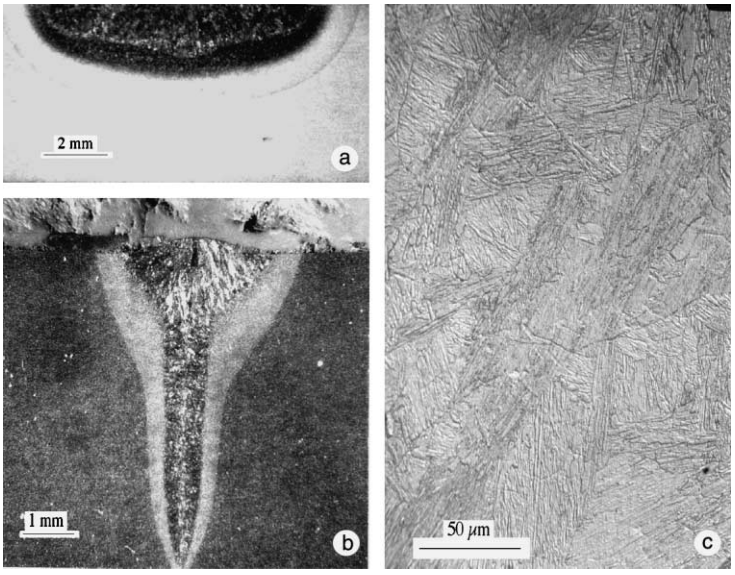

Fig. 1. (a)–(c) BATMAN IID: typical aspects of GTAW (a) and EBW (b) pools. The structure of the MZ of the GTAW weld is shown in (c).

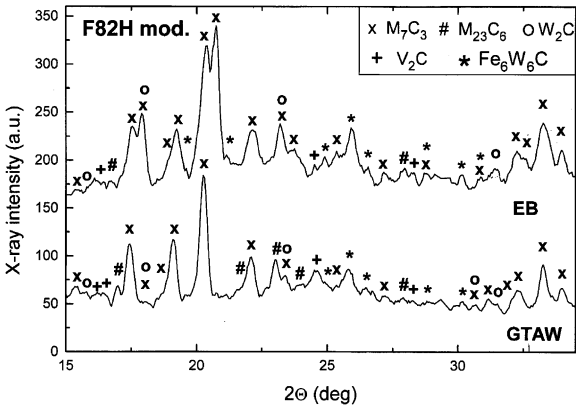

Fig. 2. F82H mod.: XRD spectra of the particles extracted from the MZ of GTAW and EB welds. Each type of carbide present in the mixture of particles gives rise to a set of diffraction lines and the XRD patterns are the overlapping of them. Markers indicate the reflections of the same set.

The PWHT is 1 h at 760 °C, i.e. the treatment that gave the best results for all the examined steel. In as-welded condition the central zone (MZ) exhibits hardness values typical of a martensitic structure. The mean hardness is 475 kgf/mm^2 (HV0.1) and decreases to 260 kgf/mm^2 after the heat treatment. After PWHT the scattering of data decreases too. Average microhardness values of all the investigated alloys in the MZ of GTAW and EB welds are reported in Table 3. Generally the MZ of EB welds show a slightly higher hardness than those of GTAW welds, this could be due to the relative higher amounts of M_7C_3 carbides, which produce secondary hardening in Cr martensitic steels. As shown in Fig. 2 for F82H mod., the relative amount of M_7C_3 carbides with respect $M_{23}C_6$ carbides is higher in the EB than in the GTAW weld.

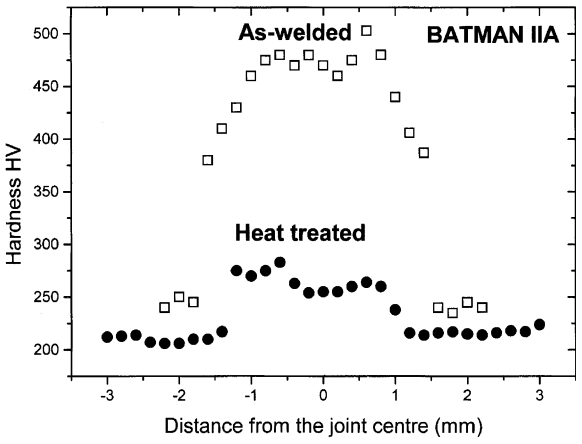

Fig. 3. BATMAN IIA: microhardness trends across an EB weld before and after the PWHT of 1 h at 760 °C.

Table 3
Average values of the microhardnesses HV measured across the molten zones of GTAW and EBW joints before and after the post-welding heat treatment of 1 h at 760 °C

Alloy	GTAW		EB	
	As-welded	Heat treated	As-welded	Heat treated
BATMAN IIA	470	290	475	260
BATMAN IID	435	275	480	255
BATMAN IIC	420	250	440	240
F82H mod.	400	265	410	220

The comparison between the microhardness values in the MZ after PWHT (Table 3) and those of the base materials (Table 2) indicates that the original characteristics are substantially, even if not completely, recovered after the treatment of 1 h at 760 °C.

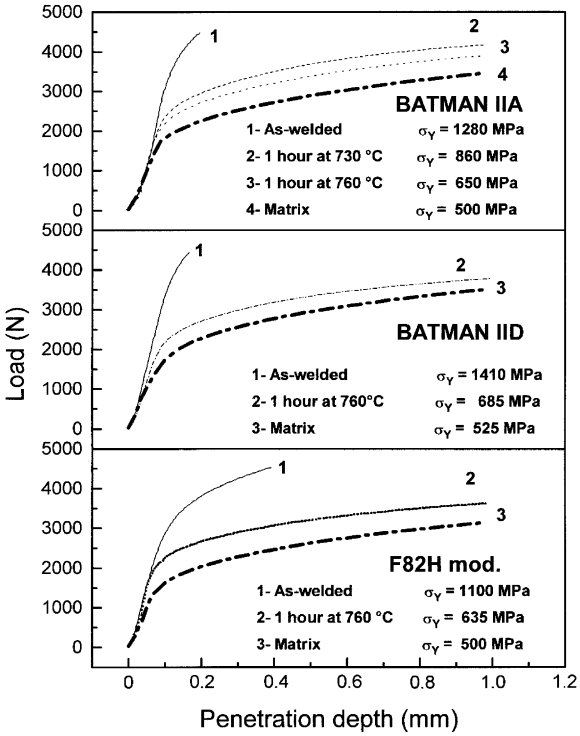

Fig. 4. Load–penetration curves obtained by FIMEC tests on the MZ of GTAW welds in BATMAN IIA, BATMAN IID and F82H mod. steels before and after 1 h at 760 °C, the PWHT that gives the best results. The curves of base materials are reported for comparison. In the case of BATMAN IIA the curve obtained after another treatment (1 h at 730 °C) are plotted to show the effectiveness of FIMEC method to determine the best PWHT.

This result is confirmed by FIMEC tests performed on GTAW welds. Fig. 4 shows the evolution of the load–penetration curves and of the values of yield stress ($\sigma_Y = q_Y/3$) determined from them for some investigated welded pools before and after PWHT. The curves obtained from the base materials are reported for comparison.

In as-welded condition the yield stresses in MZ result increased compared to the matrix values by a factor ~2.6 for BATMAN IIA, ~2.7 for BATMAN IID and 2.2 for F82H mod. steels. After the PWHT of 1 h at 760 °C, σ_Y decreases even if they do not reach the typical values of parent materials. In fact, the yield stresses of all examined steels remain ~1.3 times higher than those of the matrix. Other heat treatments gave worst results; an example is shown in Fig. 4 for BATMAN IIA. It is worth noting that the 'optimised' PWHT of Ti-bearing alloys, must be performed at temperature higher than the one chosen for the tempering of base materials.

4. Conclusions

GTA and EB methods were exploited to realise welding pools on four RA martensitic steels plates. Morphology of the welds has been investigated and described by means of optical microscopy. The structure of the MZ in GTA and EB welds and the precipitates have been identified by XRD. The relative amounts of Cr-rich carbides, M_7C_3 and $M_{23}C_6$ (M = Cr, Fe), depend on the welding techniques since they involve different cooling rates. M_7C_3 represents the most abundant species for both welding methods. A lesser quantity of $M_{23}C_6$ was revealed in the MZ of GTAW joints whereas traces of $M_{23}C_6$ are just present in EB welds. The different relative amounts of Cr-rich carbides in GTA and EB welds can explain the slightly higher hardness of MZ in EB joints.

The examined alloys have been submitted to different PWHT in a range of temperatures of ±30 °C around those of standard tempering for times of 0.5 and 1 h. Microhardness measurements across the joints and FIMEC tests directly in the MZ showed that a rather good recovery of original mechanical properties is achieved after 1 h at 760 °C.

Acknowledgements

The authors are grateful to Mr Piero Plini and Mr Benedetto Iacovone for their assistance in FIMEC tests.

References

[1] A. Hishinuma, A. Kohyama, R.L. Klue, D.S. Gelles, W. Dietz, K. Ehrlich, J. Nucl. Mater. 258–263 (1998) 193.
[2] E. Daum, K. Ehrlich, M. Schirra, FZKA-report no. 5848, 1997.
[3] K. Ehrlich, E.E. Bloom, T. Kondo, J. Nucl. Mater. 283–287 (2000) 79.
[4] A. Alamo, A. Castaing, A. Fontes, P. Wident, J. Nucl. Mater. 283–287 (2000) 1192.
[5] T. Sawai, K. Shiba, A. Hishinuma, J. Nucl. Mater. 283–287 (2000) 657.
[6] J. Rensman, E.V. van Osch, M.G. Horsten, D.S. d'Hulst, J. Nucl. Mater. 283–287 (2000) 1201.
[7] N. Inoue, T. Muroga, A. Nishimura, T. Nagasaka, O. Motojima, S. Uchida, H. Yabe, K. Oguri, Y. Nishi, Y. Katoh, A. Kohyama, J. Nucl. Mater. 283–287 (2000) 1187.
[8] K. Schleisiek, T. Lechler, L. Schaeffler, P. Weimar, J. Nucl. Mater. 283–287 (2000) 1196.
[9] L. Pilloni, F. Attura, A. Calza-Bini, G. De Santis, G. Filacchioni, A. Carosi, S. Amato, J. Nucl. Mater. 258–263 (1998) 1329.
[10] G. Filacchioni, E. Casagrande, U. De Angelis, G. De Santis, D. Ferrara, L. Pilloni, J. Nucl. Mater. 271&272 (1999) 445.
[11] P. Gondi, R. Montanari, A. Sili, S. Foglietta, A. Donato, G. Filacchioni, Fus. Technol. (1996) 1607.
[12] A. Donato, P. Gondi, R. Montanari, F. Moreschi, A. Sili, S. Storai, J. Nucl. Mater. 258–263 (1998) 446.